Chemical Science

EDGE ARTICLE

Check for updates

Catalytic enantioselective synthesis of macrodiolides and their application in chiral recognition†

Wanlong Xiao, [ID] Yuhao Mo, [ID] Jing Guo, [ID] Zhishan Su, [ID] Shunxi Dong [ID] * and Xiaoming Feng [ID] *

New types of C_2-symmetric chiral macrodiolides are readily obtained *via* chiral *N,N'*-dioxide-scandium(III) complex-promoted asymmetric tandem Friedel–Crafts alkylation/intermolecular macrolactonization of *ortho*-quinone methides with C3-substituted indoles. This protocol provides an array of enantioenriched macrodiolides with 16, 18 or 20-membered rings in moderate to good yields with high diastereoselectivities and excellent enantioselectivities through adjusting the length of the tether at the C3 position of indoles. Density functional theory calculations indicate that the formation of macrocycles is more favorable than that of 9-membered-ring lactones in terms of kinetics and thermodynamics. The potential utility of these intriguing chiral macrodiolide molecules is demonstrated in the enantiomeric recognition of aminols and chemical recognition of metal ions.

Introduction

Macrocycles are one of the most popular structural motifs in many natural products and commercial drugs.[1] In particular, macrolactones have received considerable and continuous attention due to their unique structure and remarkable biological activities (Scheme 1a).[2] In addition, some recent examples illustrated that macrolactones are good candidates as host molecules in supramolecular chemistry, further highlighting the importance of this type of compound.[3] In the above context, the development of feasible and facile routes to macrocycles holds a pivotal position. Therefore, tremendous efforts have been devoted over the past few decades and many kinds of methods have been established including macrolactonization, ring-closing metathesis, intramolecular cross-coupling, the Nozaki–Hiyama–Kishi reaction, the Horner–Wadsworth–Emmons reaction, the click reaction, *etc.*[4] Among them, the most frequently used synthetic strategy toward macrolactones is macrolactonization, which mainly relies on acyl activation with special requirements involving high dilution conditions, structural pre-organization and the use of exotic coupling reagents.[5] Nevertheless, the exploration of concise and efficient synthetic methods to construct new

kinds of macrolactones not only expands their chemical diversity, but also accelerates the discovery of new functions of such compounds.
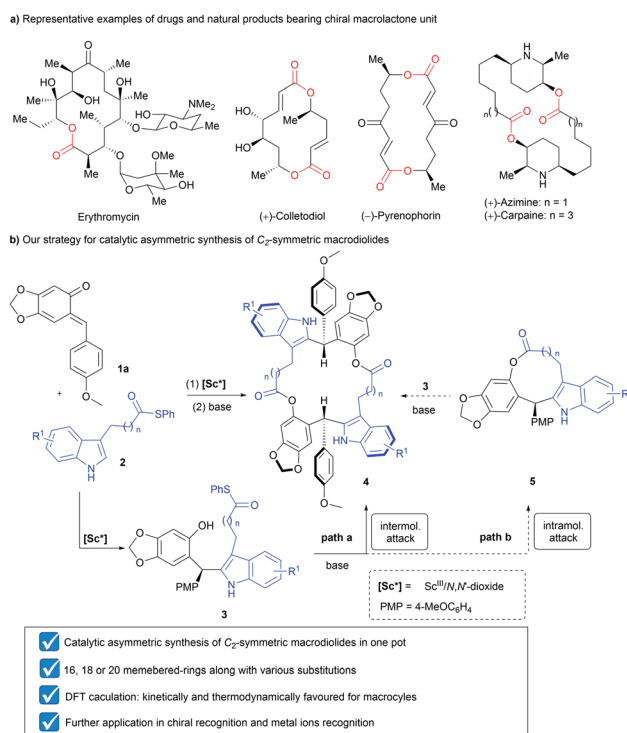
Scheme 1 (a) Representative examples of drugs and natural products bearing a chiral macrolactone unit; (b) our strategy for catalytic asymmetric synthesis of C_2-symmetric macrodiolides.

Key Laboratory of Green Chemistry & Technology, Ministry of Education, College of Chemistry, Sichuan University, Chengdu 610064, China. E-mail: dongs@scu.edu.cn; xmfeng@scu.edu.cn

Molecular chirality plays a crucial role in chemistry, biology, and drug development since enantiomeric molecules have distinct interactions with another chiral object.[6] Accordingly, the chirality of macrolactones is closely associated with their biological activities and enantiomeric recognition properties.[7] However, most of the known synthetic strategies towards C_2-symmetric chiral macrodiolides are linear multistep synthesis approaches, which need orthogonally protected building blocks and/or previously constructed stereogenic centers.[8] Although asymmetric catalysis[9] is the most effective and powerful method to construct chiral molecules, this strategy has been seldom used in the synthesis of chiral macrolactones probably due to the lack of reliable methods.[10]

As part of our continuous efforts in expanding the utility of chiral N,N'-dioxide-metal complexes[11] and inspired by the versatile roles played by ortho-quinone methides (o-QMs)[12] in organic synthesis, we envisioned that rational design of a substrate would provide a potential solution to the above issue. As depicted in Scheme 1b, indoles 2 bearing an alkyl thioester unit at the C3-position were chosen. We envisaged that they can react with ortho-quinone methide 1a to afford chiral diarylindolylmethane intermediate 3 via Friedel–Crafts alkylation.[13] Then, under basic conditions, the forming phenol group in compound 3 undergoes either intramolecular or intermolecular nucleophilic attack of the alkyl thioester to form 9 or 18-membered-ring lactones 5 or 4. Arising from the large strain[14] of the 9-membered ring with the rigid indole skeleton, we assumed that 18-membered-ring lactone 4 was more likely to form in this process.[15] Herein, we wish to report our endeavor along this line. The chiral N,N'-dioxide-scandium(III) complex was found to be efficient in promoting the tandem Friedel–Crafts alkylation/intermolecular macrolactonization reaction, providing chiral 16, 18 or 20-membered-ring macrolactones in moderate to good yields with high diastereoselectivities and excellent enantioselectivities. Theoretical calculations disclosed that the formation of macrocycles 4 was kinetically and thermodynamically favored compared to the generation of lactones 5 with the 9-membered ring. The constantly excellent ee values of chiral macrodiolides 4 were rationalized by the formation of their meso counterparts in the macrolactonization step. The application of these optically active macrodiolides was demonstrated in the enantiomeric recognition[16] of aminols and chemical recognition of metal ions.[17]

Results and discussion

Initially, we chose ortho-quinone methide 1a and 3-indolepropanethioate 2a as model substrates to optimize the Friedel–Crafts alkylation reaction conditions (Table 1). The screening of a series of metal salts combined with chiral N,N'-dioxide L_3-$PiPr_2$ (Table 1, entries 1–4) indicated that many Lewis acids enabled accelerating the Friedel–Crafts alkylation reaction except $Zn(OTf)_2$ (see Tables S1–S5 in the ESI,† pages 6–8). The use of $Al(OTf)_3$ as the central metal led to a racemic product 3aa in 30% yield (Table 1, entry 2). In comparison, rare-earth metals afforded good enantioselectivities, and $Sc(OTf)_3$ was a good choice, providing the desired product 3aa in 96% yield

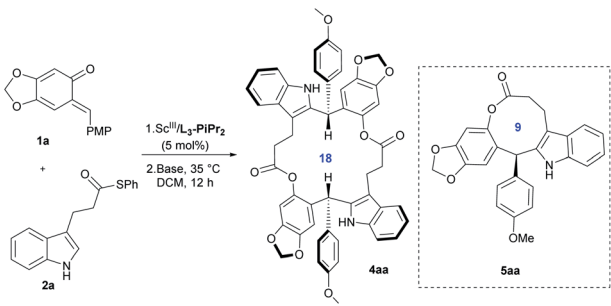**Table 1** Optimization of the Friedel–Crafts alkylation reaction conditions[a]
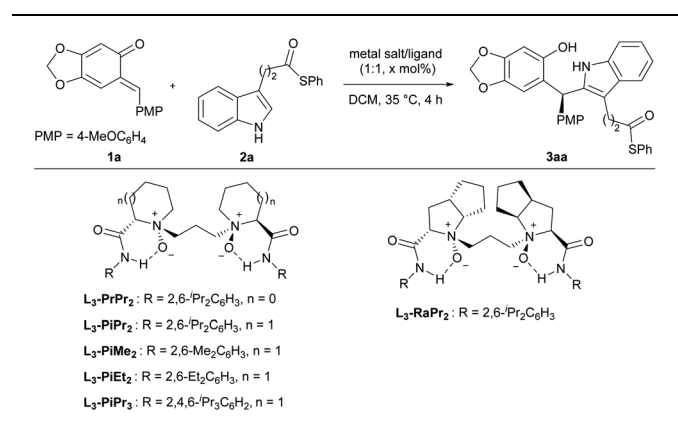
Entry	Metal salt	Ligand	x (mol%)	Yield[b] (%)	ee[c] (%)
1	$Zn(OTf)_2$	L_3-$PiPr_2$	10	n.r.	—
2	$Al(OTf)_3$	L_3-$PiPr_2$	10	30	0
3	$Y(OTf)_3$	L_3-$PiPr_2$	10	72	71
4	$Sc(OTf)_3$	L_3-$PiPr_2$	10	96	93
5	$Sc(OTf)_3$	L_3-$PrPr_2$	10	95	73
6	$Sc(OTf)_3$	L_3-$RaPr_2$	10	83	84
7	$Sc(OTf)_3$	L_3-$PiEt_2$	10	95	90
8	$Sc(OTf)_3$	L_3-$PiMe_2$	10	99	83
9	$Sc(OTf)_3$	L_3-$PiPr_3$	10	95	86
10	$Sc(OTf)_3$	L_3-$PiPr_2$	5	99	93
11	$Sc(OTf)_3$	L_3-$PiPr_2$	2.5	39	56

[a] All reactions were carried out with 1a (0.1 mmol), 2a (0.1 mmol), and metal salt/ligand (1 : 1, x mol%) in dichloromethane (DCM, 1.0 mL) at 35 °C for 4 h. [b] Yield of the isolated product. [c] Determined by HPLC analysis on a chiral stationary phase. n.r. = no reaction.

with 93% ee (Table 1, entry 4). Next, the influence of chiral N,N'-dioxide ligands was studied (Table 1, entries 4–9). Compared with L_3-$PiPr_2$ derived from S-pipecolic acid, L-proline-derived L_3-$PrPr_2$ and L-ramipril-based L_3-$RaPr_2$ produced adduct 3aa in lower enantioselectivities (Table 1, entries 4–6, 73% ee and 84% ee vs. 93% ee). Reducing the steric hindrance at the 2,6-position of aniline in the ligands resulted in an obvious decrease in enantioselectivity (Table 1, entries 7 and 8 vs. entry 4). Installing another isopropyl substitution at the para-position of the phenyl group of the amide moiety had an adverse effect on chiral control (Table 1, entry 9, 86% ee). Both the yield and enantioselectivity were maintained when the reaction was carried out with 5 mol% catalyst loading (Table 1, entry 10). However, upon further decreasing the catalyst loading from 5 mol% to 2.5 mol%, the desired product 3aa was obtained in poor reactivity and enantioselectivity (Table 1, entry 11 vs. entry 10). Consequently, the optimized reaction conditions for the Friedel–Crafts alkylation reaction involved the use of 5 mol% L_3-$PiPr_2$/$Sc(OTf)_3$ as the catalyst in DCM at 35 °C for 4 hours. Under such conditions, the desired product 3aa was isolated in 99% yield and 93% ee (Table 1, entry 10).

After establishing the optimized reaction conditions for the Friedel–Crafts alkylation reaction (Table 1, entry 10), we carried
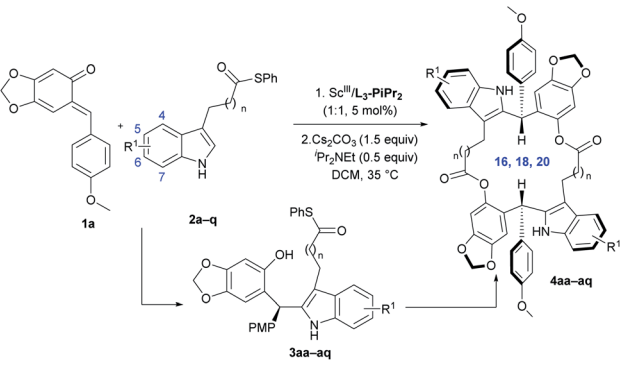
Table 2 Optimization of the macrolactonization reaction conditions[a]

Entry	Base	Yield[b] (%)	dr[c]	ee[d] (%)
1	DMAP (1.0 equiv.)	47	92 : 8	99
2	DIPEA (1.0 equiv.)	Trace	—	—
3	Cs$_2$CO$_3$ (1.0 equiv.)	55	92 : 8	99
4	Cs$_2$CO$_3$ (2.0 equiv.)	67	92 : 8	99
5	Cs$_2$CO$_3$ (3.0 equiv.)	58	92 : 8	99
6	Cs$_2$CO$_3$ (1.5 equiv.) DIPEA (0.5 equiv.)	70	93 : 7	99

[a] All reactions were carried out with **1a** (0.1 mmol), **2a** (0.1 mmol), and Sc(OTf)$_3$/**L$_3$-PiPr$_2$** (1 : 1, 5 mol%) in DCM (1.0 mL) at 35 °C for 4 h, and then base was added, and the resulting reaction mixture was stirred at 35 °C for 12 h. [b] Yield of isolated product **4aa**. [c] Determined by ^{1}H NMR analysis. [d] Determined by UPC^2 analysis on a chiral stationary phase. DMAP = 4-dimethylaminopyridine, DIPEA = N,N-diisopropylethylamine.

out the study on the lactonization reaction using the same substrates **1a** and **2a** with a one-pot procedure. It was found that bases showed a crucial influence on the reactivity of the ring-closing reaction (see Tables S6–S9 in the ESI,† pages 8–11). In this ring-closing process, the 18-membered-ring macrodiolide product **4aa** was preferably generated instead of the 9-membered ring product **5aa** in terms of kinetics and thermodynamics, which was proved by the density functional theory calculations in the following part. 4-Dimethylamino-pyridine (DMAP) promoted the ring-closing process smoothly, delivering 18-membered-ring macrodiolide **4aa** as the major product (Table 2, entry 1, 47% yield with 92 : 8 dr and 99% ee). It should be noted that the other diastereomer was a *meso* compound, which was identified by X-ray crystal structure analysis.[18a] Comparably, the lactonization reaction didn't occur in the presence of DIPEA (Table 2, entry 2). An inorganic base, for instance Cs$_2$CO$_3$, provided the best results, and the 18-membered-ring product **4aa** was isolated in 55% yield with comparable dr and ee values (Table 2, entry 3). The addition of 2 equivalents of Cs$_2$CO$_3$ led to a higher yield (Table 2, entry 4, 67%). No better result was obtained by further increasing the amount of Cs$_2$CO$_3$ (Table 2, entry 5). The subsequent investigation indicated that the use of a mixture of Cs$_2$CO$_3$ (1.5 equiv.) and DIPEA (0.5 equiv.) afforded a slightly higher yield (Table 2, entry 6, 70%). Therefore, the optimal reaction conditions for the overall reaction were established as 5 mol% **L$_3$-PiPr$_2$**/Sc(OTf)$_3$ as a catalyst in DCM at 35 °C for 4 hours, and then 1.5 equivalents of Cs$_2$CO$_3$ and 0.5 equivalents of DIPEA were added in DCM at 35 °C for 12 hours.

With the optimized reaction conditions (Table 2, entry 6) in hand, the substrate scope of indoles was explored (Table 3). A series of indoles **2** with different substituents could react with *ortho*-quinone methide **1a** smoothly, regardless of the electronic nature and the position of substituents at the aromatic ring (Table 3, entries 1–17). In detail, both electron-withdrawing and electron-donating substituents on the 4, 5 or 6-positions of indoles could give the corresponding 18-membered-ring products **4ab–4ao** in moderate to good yields (47–75%), high diastereoselectivities (91 : 9 to 94 : 6 dr) and excellent enantioselectivity (in all cases, 99% ee). We performed two parallel reactions for each substrate, and thereby Friedel–Crafts alkylation products **3** were isolated and characterized as well. The configuration of chiral product **3as** (see Table S10, entry 19 in the ESI,† page 13) was determined to be (S) by X-ray crystal
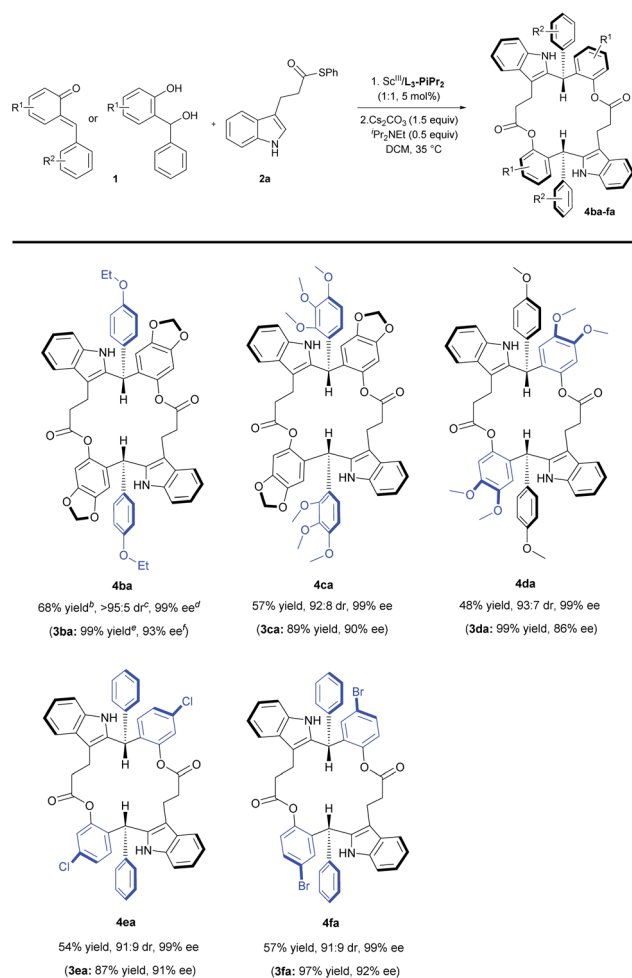
Table 3 Substrate scope for the reaction of indoles[a]

Entry	R^1, n	**3**			**4**		
		Yield[b] (%)	ee[c] (%)	Yield[d] (%)	dr[e]	ee[f] (%)
1	H, n = 1	99 (**3aa**)	93	70 (**4aa**)	93 : 7	99
2	4-Cl, n = 1	95 (**3ab**)	93	63 (**4ab**)	94 : 6	99
3	4-F, n = 1	91 (**3ac**)	91	58 (**4ac**)	93 : 7	99
4	4-Me, n = 1	99 (**3ad**)	93	63 (**4ad**)	93 : 7	99
5	5-Br, n = 1	99 (**3ae**)	91	48 (**4ae**)	91 : 9	99
6	5-Cl, n = 1	97 (**3af**)	92	47 (**4af**)	91 : 9	99
7	5-F, n = 1	90 (**3ag**)	91	57 (**4ag**)	93 : 7	99
8	5-Me, n = 1	99 (**3ah**)	93	60 (**4ah**)	91 : 9	99
9	5-OMe, n = 1	93 (**3ai**)	92	69 (**4ai**)	92 : 8	99
10	6-Br, n = 1	96 (**3aj**)	91	75 (**4aj**)	93 : 7	99
11	6-Cl, n = 1	99 (**3ak**)	94	66 (**4ak**)	93 : 7	99
12	6-F, n = 1	98 (**3al**)	94	60 (**4al**)	93 : 7	99
13	6-Me, n = 1	95 (**3am**)	92	59 (**4am**)	92 : 8	99
14	7-Cl, n = 1	97 (**3an**)	92	70 (**4an**)	94 : 6	99
15	7-Me, n = 1	97 (**3ao**)	90	50 (**4ao**)	93 : 7	99
16	H, n = 2	97 (**3ap**)	94	45 (**4ap**)	90 : 10	99
17	H, n = 0	99 (**3aq**)	97	58 (**4aq**)	>95 : 5	99

[a] Reaction conditions for products **3** : **1a** (0.1 mmol), **2** (0.1 mmol), and Sc(OTf)$_3$/**L$_3$-PiPr$_2$** (1 : 1, 5 mol%) in DCM (1.0 mL) at 35 °C. Reaction conditions for products **4** : **1a** (0.1 mmol), **2** (0.1 mmol), and Sc(OTf)$_3$/**L$_3$-PiPr$_2$** (1 : 1, 5 mol%) in DCM (1.0 mL) at 35 °C, and then Cs$_2$CO$_3$ (1.5 equiv.) and [i]Pr$_2$NEt (0.5 equiv.) were added, and the resulting reaction mixture was stirred at 35 °C. [b] Yield of the isolated product. [c] Determined by HPLC analysis on a chiral stationary phase. [d] Yield of the isolated product over two steps. [e] Determined by ^{1}H NMR analysis. [f] Determined by UPC^2 analysis on a chiral stationary phase.

structure analysis.[18b] Notably it's interesting to find that regardless of the enantioselectivities (90–97% ee) of the intermediates **3**, the enantiomeric excess of 18-membered-ring products **4** was always 99% ee. Generally, indoles with electron-donating substituents provided slightly higher yields than those with electron-withdrawing substituents (Table 3, entry 4 vs. entries 2 and 3; entries 8 and 9 vs. entries 5–7). In contrast, the yield of 6-methyl substituted indole **2m** was lower (Table 3, entry 13 vs. entries 10–12). Besides, moderate yields with excellent diastereoselectivities and enantioselectivities were obtained for 7-chlorine and methyl substituted indoles (Table 3, entries 14 and 15). To our delight, upon increasing or decreasing the carbon chain length in indole substrates **2p** and **2q**, the reactions were equally good, generating the

corresponding 20-membered-ring product **4ap** and 16-membered-ring product **4aq** in decent yields with high diastereo- and enantioselectivities (Table 3, entries 16 and 17). The absolute configuration of product **4ab** was confirmed to be (S,S) by X-ray diffraction analysis[18c] and the configurations of all other examples were assigned by comparing their CD spectra with that of **4ab**. Subsequently, the substrate scope of ortho-quinone methides was tested (Table 4). Representative ortho-quinone methides **1** were subjected to the standard conditions, and the reaction occurred smoothly to afford the corresponding 18-membered-ring products (**4ba–4da**) in good yields (48–68%), high diastereoselectivities (92 : 8 to >95 : 5 dr) and excellent enantioselectivity (99% ee). When ortho-hydroxybenzyl alcohols were employed as the precursor of o-QMs, they could transform into the o-QMs in situ and react with indole **2a** efficiently, yielding the desired macrodiolides **4ea–4fa** in medium yields (54% and 57%) with a high dr value (91 : 9) and excellent ee value (99% ee).
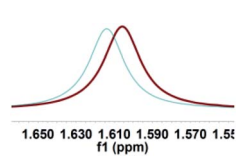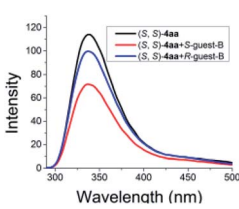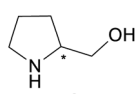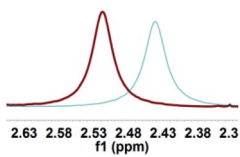
In order to evaluate the synthetic utility of this catalytic system, a gram-scale synthesis of **4aa** was carried out (Scheme 2, left). Under the optimized reaction conditions, ortho-quinone methide **1a** (4.0 mmol, 1.03 g) reacted smoothly with 3-indole-propanethioate **2a** (4.0 mmol, 1.13 g), affording the desired product **4aa** in 63% yield (1.07 g) with 93 : 7 dr and 99% ee.

As illustrated in Scheme 2, right, the chiral macrodiolide product (S,S)-**4ab** possesses a C_2-symmetric structure, wherein two carbonyl oxygens orient up with a distance of 3.94 Å, and two PMP groups point down. The distance between the two hydrogens located at stereogenic centers is approximately 4.05 Å. In view of such a chiral macrocyclic structure bearing hydrogen-bond donor and acceptor sites, we subsequently investigated its potential application in chiral recognition. Firstly, the chiral discrimination abilities of chiral macrodiolide **4aa** (99% ee) were evaluated with enantiomers of chiral amines, alcohols, amino alcohols, alcohol esters, etc. Because the strength of interaction between enantiomers of chiral objects and chiral macrocycles is different, the chiral recognition effect is significantly different (see Tables S13 and S14 in the ESI,† pages 98–114). The preliminary results indicated that chiral macrodiolide **4aa** showed enantiodifferentiation of the enantiomers of amines and amino alcohols (Table 5, entries 1–4,

Table 4 Substrate scope for the reaction of ortho-quinone methides or ortho-hydroxybenzyl alcohols[a]

4ba
68% yield[b], >95:5 dr[c], 99% ee[d]
(**3ba**: 99% yield[e], 93% ee[f])

4ca
57% yield, 92:8 dr, 99% ee
(**3ca**: 89% yield, 90% ee)

4da
48% yield, 93:7 dr, 99% ee
(**3da**: 99% yield, 86% ee)

4ea
54% yield, 91:9 dr, 99% ee
(**3ea**: 87% yield, 91% ee)

4fa
57% yield, 91:9 dr, 99% ee
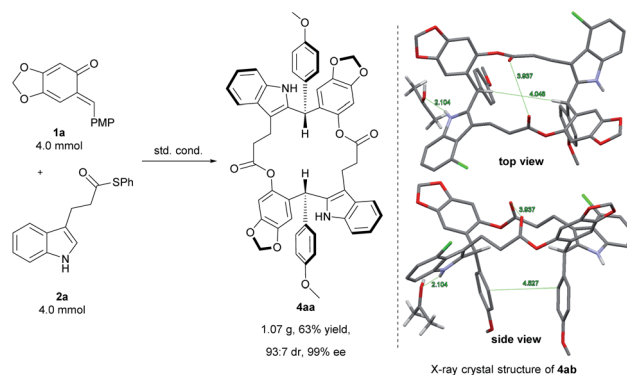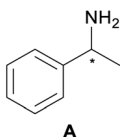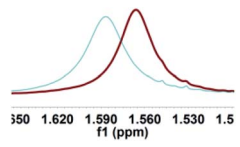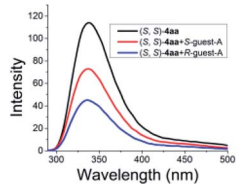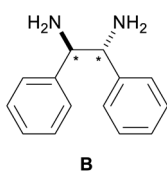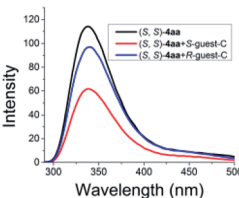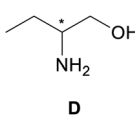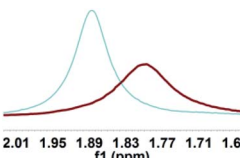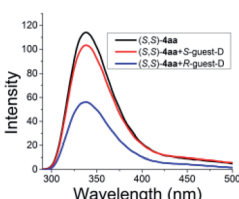(**3fa**: 97% yield, 92% ee)

[a] Reaction conditions of products **3** : **1** (0.1 mmol), **2a** (0.1 mmol), and Sc(OTf)$_3$/**L$_3$-PiPr$_2$** (1 : 1, 5 mol%) in DCM (1.0 mL) at 35 °C. Reaction conditions of products **4** : **1** (0.1 mmol), **2a** (0.1 mmol), and Sc(OTf)$_3$/**L$_3$-PiPr$_2$** (1 : 1, 5 mol%) in DCM (1.0 mL) at 35 °C, and then Cs$_2$CO$_3$ (1.5 equiv.) and ^{i}Pr$_2$NEt (0.5 equiv.) were added, and the resulting reaction mixture was stirred at 35 °C. [b] Yield of the isolated product over two steps. [c] Determined by ^{1}H NMR analysis. [d] Determined by UPC^2 analysis on a chiral stationary phase. [e] Yield of the isolated product. [f] Determined by HPLC analysis on a chiral stationary phase.

Scheme 2 Gram-scale asymmetric synthesis and X-ray crystal structure of **4ab**.

Table 5 Chiral recognition of (*S,S*)-**4aa** toward guests **A**–**D** by ^{1}H NMR analysis and fluorescence analysis

Entry	Guest	Chiral recognition by ^{1}H NMR analysis[a]		Chiral recognition by fluorescence analysis[d]	
		Spectrum[b] (^{1}H NMR)	$\Delta\delta^c$ (ppm)	Spectrum (fluorescence)[e]	ef[f]
1	**A**		0.021		1.68 (0.60)
2[g]	**B**		0.008		3.02 (0.33)
3	**C**		0.076		2.92 (0.34)
4	**D**		0.087		5.46 (0.18)

[a] All samples were prepared by mixing (*S,S*)-**4aa** and guests **A**–**D** in NMR tubes [36 mM (*S,S*)-**4aa** and 72 mM guests **A**–**D** in 0.7 mL of CDCl$_3$]. ^{1}H NMR data were collected on an NMR spectrometer (400 MHz) at 25 °C. [b] The N–H signals of *S*-guests **A**–**D** with (*S,S*)-**4aa** (blue) *vs.* *R*-guests **A**–**D** with (*S,S*)-**4aa** (red). [c] $\Delta\delta$ of the N–H group of guests **A**–**D**. [d] Fluorescence responses of (*S,S*)-**4aa** (0.5 mM) toward guests **A**–**D** (1 mM) in CH$_3$CN (λ_{ex} = 265 nm, slits: 2.5/20 nm). [e] Fluorescence spectra of (*S,S*)-**4aa** (black) *vs.* (*S,S*)-**4aa** with *S*-guests-**A**–**D** (red) *vs.* (*S,S*)-**4aa** with *R*-guests-**A**–**D** (blue). [f] The enantiomeric fluorescence difference ratio, ef = $(I_0 - I_R)/(I_0 - I_S)$. (λ_{em} = 335.2 nm). [g] The configuration of *S*-guest-**B** is (1*S*,2*S*) and the configuration of *R*-guest-**B** is (1*R*,2*R*).

left). The best result was obtained with 36 mM chiral macrodiolide **4aa** and 72 mM 2-aminobutanol in deuterated chloroform, and the corresponding $\Delta\delta$ value was 0.087 ppm (Table 5, entry 4). The subsequently enantioselective fluorescence recognition studies suggested that chiral macrodiolide **4aa** could serve as a chiral receptor to discriminate the enantiomers of 2-aminobutanol, and the addition of chiral macrodiolide **4aa** into the solution of (*S*)-2-aminobutanol in CH$_3$CN led to a slight fluorescence quenching. In sharp contrast, an obvious fluorescence quenching was observed in the case of (*R*)-2-aminobutanol. The enantiomeric fluorescence difference ratio, ef = $(I_0 - I_R)/(I_0 - I_S)$, was as high as 5.46. Comparably, the acyclic intermediate **3aa** showed much less discriminating ability (1.45 ef value) under the same conditions (see Table S14 in the ESI,† pages 113 and 114), indicating the beneficial effect of a relatively more rigid macrocyclic structure. For the fluorescence quenching chiral recognition probe, many fluorescence quenching processes followed the Stern–Volmer equation: $I_0/I = 1 + K_{SV}[Q]$. Here I and I_0 are the fluorescent intensity of the

fluorophore (*S,S*)-**4aa** with and without the quencher, [Q] is the concentration of the quencher, and K_{SV} is the Stern–Volmer constant.[19] For guest-**B** (1,2-diphenyl-1,2-ethanediamine), the Stern–Volmer constant of (*S,S*)-**4aa** was 326.53 M^{-1} [$K_{SV}(S - S)$] in the presence of *S*-guest-**B** and 275.09 M^{-1} [$K_{SV}(S - R)$] in the presence of *R*-guest-**B**. The ratio of the Stern–Volmer constant [$K_{SV}(S - S)$]/[$K_{SV}(S - R)$] was 1.19 (see Table S15 in the ESI,† page 125). Thus, *S*-guest-**B** quenched the fluorescence of (*S,S*)-**4aa** more efficiently than *R*-guest-**B**. In addition, considering potential recognition ability of macrocycles towards metal ions, we investigated the recognition effect of macrodiolide (*S,S*)-**4aa** in acetonitrile by UV-vis absorption spectroscopy and fluorescence spectrum analysis (see Fig. S1–S4 in the ESI,† pages 129 and 130). The addition of Fe(OTf)$_2$ to the solution of (*S,S*)-**4aa** lowered the fluorescence intensity of (*S,S*)-**4aa** (Fig. 1). Furthermore, the addition of Fe(OTf)$_3$ or Cu(OTf)$_2$ to the solution of (*S,S*)-**4aa** led to a redshift and enhancement of fluorescence. This process was accompanied by color changes visible to the naked eye (see Fig. S5–S7 in the ESI,† page 131). The
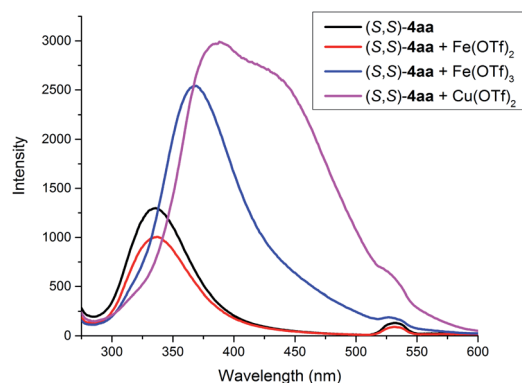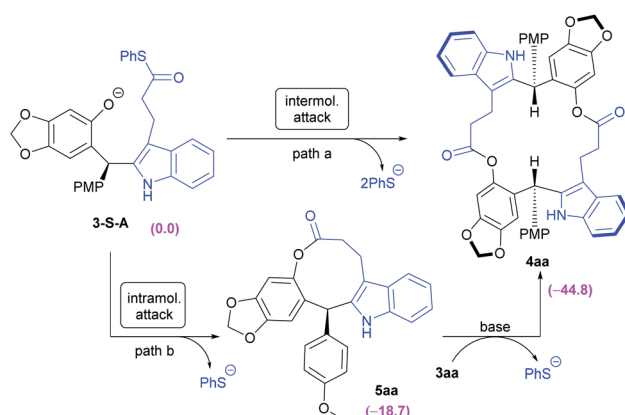
Fig. 1 Fluorescence spectra of (*S*,*S*)-**4aa** at 5×10^{-5} M with or without a metal precursor (5×10^{-5} M) in CH$_3$CN. (λ_{ex} = 265 nm, slits: 2.5/20 nm).

experimental results showed that macrodiolide product (*S*,*S*)-**4aa** could selectively recognize Fe^{2+}, Fe^{3+}, Cu^{2+}.

To gain insight into the formation of the eighteen-membered-ring product (*S*,*S*)-**4aa**, DFT calculation was performed at the B3LYP-D3(BJ)/6-31G(d,p) (SMD, CH$_2$Cl$_2$) theoretical level. Two pathways (Scheme 3, path a and b) were investigated, wherein the intramolecular or intermolecular cyclization reactions were involved, respectively. As shown in Scheme 3, (*S*)-**3aa** underwent a deprotonation process with a basic reagent (*e.g.* Cs$_2$CO$_3$), producing the corresponding anion **3-S-A**. The eighteen-membered-ring product (*S*,*S*)-**4aa** could be generated through intermolecular attack of the phenoxy anion at the C atom of the carbonyl group in another molecule (path a). In addition, if an intramolecular cyclization reaction occurs, the nine-membered-ring intermediate (*S*)-**5aa** was afforded with the release of a SPh anion (path b). Molecular modeling indicated that the nine-membered-ring (*S*)-**5aa** adopted a boat-like conformation (see Fig. S10 in the ESI,† page 133), in which two aromatic rings were connected by the planar ester group as well as a –(CH$_2$)$_2$– chain. This less stable rigid structure rendered (*S*)-**5aa** prone to undergoing a ring-opening reaction with another (*S*)-**3aa** to yield the final eighteen-

membered-ring product (*S*,*S*)-**4aa**. Compared to (*S*)-**5aa** with a nine-membered ring ($\Delta G = -18.7$ kcal mol^{-1}), (*S*,*S*)-**4aa** has a lower relative Gibbs free energy of formation ($\Delta G = -44.8$ kcal mol^{-1}), suggesting that the eighteen-membered-ring product (*S*,*S*)-**4aa** was more stable thermodynamically (see Fig. S9 and S10 in the ESI,† pages 132 and 133).

In terms of the activation energy barrier, the activation energy barrier of the initial intermolecular attack in path a was 7.0 kcal mol^{-1} lower than that of the ring-closure reaction for nine-membered-ring product (*S*)-**5aa** in path b (2.4 *vs.* 9.4 kcal mol^{-1}). These results indicated that it was more possible for (*S*)-**3aa** to undergo intermolecular reaction *via* path a, producing the eighteen-membered-ring product (*S*,*S*)-**4aa**. However, path b cannot be ruled out.

Moreover, to gain insights into the product distribution, the formation of mesoisomer (*R*,*S*)-**4aa** *via* path a was studied at the same theoretical level. The calculation results showed that the formation of mesoisomer (*R*,*S*)-**4aa** in the second C–O bond construction step was slightly favored over that of chiral (*S*,*S*)-**4aa** in terms of kinetics (the activation energy barrier, 6.8 kcal mol^{-1} *vs.* 13.9 kcal mol^{-1}) and thermodynamics (relative Gibbs free energy of formation ΔG: -48.4 kcal mol^{-1} *vs.* -44.8 kcal mol^{-1}), which provide a rational explanation for the excellent ee value (99% ee) of eighteen-membered-ring products **4** (see Fig. S11–S13 in the ESI,† page 134).

Conclusions

In summary, we have developed a concise and facile route to C_2-symmetric chiral macrodiolides through chiral *N*,*N*′-dioxide-scandium(III) complex-promoted asymmetric tandem Friedel–Crafts alkylation/intermolecular macrolactonization of *ortho*-quinone methides with C3-substituted indoles. An array of enantioenriched macrodiolides with 16, 18 or 20-membered rings was readily afforded in moderate to good yields with high diastereoselectivities and excellent enantioselectivities by adjusting the length of the tether at the C3 position in indoles. DFT calculation was performed to elucidate the formation process of chiral macrodiolide products and the observed excellent enantiomeric excess. The potential application of this type of chiral macrodiolide molecule in enantiomeric recognition of aminols was confirmed by NMR study and enantioselective fluorescence recognition experiments. And their chemical recognition ability of metal ions was also studied through UV-vis absorption spectroscopy and fluorescence spectrum analysis. Further bioactivity testing of macrocyclic products and the exploration of other reactions with the chiral *N*,*N*′-dioxide-metal complex are being carried out in our lab.

Conflicts of interest

There are no conflicts to declare.

Acknowledgements

Scheme 3 Reaction mechanism for the transformation from **3aa** to **4aa**.

Notes and references

1 For selected reviews: (*a*) L. A. Wessjohann, E. Ruijter, D. Garcia-Rivera and W. Brandt, *Mol. Diversity*, 2005, **9**, 171–186; (*b*) E. Marsault and M. L. Peterson, *J. Med. Chem.*, 2011, **54**, 1961–2004; (*c*) J. Mallinson and I. Collins, *Future Med. Chem.*, 2012, **4**, 1409–1438.

2 For a leading review and a selected example: (*a*) L. Katz and G. W. Ashley, *Chem. Rev.*, 2005, **105**, 499–527; (*b*) I. B. Seiple, Z. Y. Zhang, P. Jakubec, A. Langlois-Mercier, P. M. Wright, D. T. Hog, K. Yabu, S. R. Allu, T. Fukuzaki, P. N. Carlsen, Y. Kitamura, X. Zhou, M. L. Condakes, F. T. Szczypiński, W. D. Green and A. G. Myers, *Nature*, 2016, **533**, 338–345.

3 For selected recent examples: (*a*) J. D. Wu, J. R. Lu, J. G. Liu, C. H. Zheng, Y. X. Gao, J. Hu and Y. Ju, *Sens. Actuators, B*, 2017, **241**, 931–937; (*b*) Z. Zhang, C. Q. Deng, Y. Zou and L. Chen, *J. Photochem. Photobiol., A*, 2018, **356**, 7–17; (*c*) H. X. Chai, L.-P. Yang, H. Ke, X.-Y. Pang and W. Jiang, *Chem. Commun.*, 2018, **54**, 7677–7680.

4 For selected reviews: (*a*) C. M. Madsen and M. H. Clausen, *Eur. J. Org. Chem.*, 2011, **2011**, 3107–3115; (*b*) V. Martí-Centelles, M. D. Pandey, M. I. Burguete and S. V. Luis, *Chem. Rev.*, 2015, **115**, 8736–8834; (*c*) K. T. Mortensen, T. J. Osberger, T. A. King, H. F. Sore and D. R. Spring, *Chem. Rev.*, 2019, **119**, 10288–10317; (*d*) S. Sengupta and G. Mehta, *Org. Biomol. Chem.*, 2020, **18**, 1851–1876.

5 For selected reviews: (*a*) K. C. Nicolaou, *Tetrahedron*, 1977, **33**, 683–710; (*b*) A. Parenty, X. Moreau, G. Niel and J.-M. Campagne, *Chem. Rev.*, 2013, **113**, PR1–PR40; for selected recent examples: (*c*) M. de Léséleuc and S. K. Collins, *ACS Catal.*, 2015, **5**, 1462–1467; (*d*) B. Jiang, M. Zhao, S.-S. Li, Y.-H. Xu and T.-P. Loh, *Angew. Chem., Int. Ed.*, 2018, **57**, 555–559; (*e*) C. S. Higman, D. L. Nascimento, B. J. Ireland, S. Audörsch, G. A. Bailey, R. McDonald and D. E. Fogg, *J. Am. Chem. Soc.*, 2018, **140**, 1604–1607; (*f*) Q. Zeng, K. Y. Dong, C. Pei, S. L. Dong, W. H. Hu, L. H. Qiu and X. F. Xu, *ACS Catal.*, 2019, **9**, 10773–10779; (*g*) M. Yang, X. W. Wang and J. F. Zhao, *ACS Catal.*, 2020, **10**, 5230–5235.

6 For selected books: (*a*) A. N. Collins, G. N. Sheldrake and J. Crosby, *Chirality in Industry: The Commercial Manufacture and Applications of Optically Active Compounds*, John Wiley & Sons Ltd., Chichester, 1992; (*b*) A. N. Collins, G. N. Sheldrake and J. Crosby, *Chirality in Industry II: Developments in the Commercial Manufacture and Applications of Optically Active Compounds*, John Wiley & Sons Ltd., Chichester, 1997; (*c*) K. Mislow, in *Topics in Stereochemistry*, ed. S. E. Denmark, John Wiley & Sons Inc., New York, 1999, vol. 22, pp. 1–82.

7 For selected reviews: (*a*) S. D. Appavoo, S. Huh, D. B. Diaz and A. K. Yudin, *Chem. Rev.*, 2019, **119**, 9724–9752; (*b*) K. Zheng and R. Hong, *Nat. Prod. Rep.*, 2019, **36**, 1546–1575; for selected examples: (*c*) M. Z. Gao, J. Gao, Z. L. Xu and R. A. Zingaro, *Tetrahedron Lett.*, 2002, **43**, 5001–5003; (*d*) S. Şeker, D. Barış, N. Arslan, Y. Turgut, N. Pirinççioğlu and M. Toğrul, *Tetrahedron: Asymmetry*, 2014, **25**, 411–417.

8 E. J. Kang and E. Lee, *Chem. Rev.*, 2005, **105**, 4348–4378.

9 For selected books: (*a*) *New Frontiers in Asymmetric Catalysis*, ed. K. Mikami and M. Lautens, John Wiley & Sons Inc., New York, 2007; (*b*) *Catalytic Asymmetric Synthesis*, ed. I. Ojima, John Wiley & Sons Inc., New York, 2010.

10 For a selected recent review and examples: (*a*) Y. Li, X. L. Yin and M. J. Dai, *Nat. Prod. Rep.*, 2017, **34**, 1185–1192; (*b*) A. M. Haydl and B. Breit, *Angew. Chem., Int. Ed.*, 2015, **54**, 15530–15534; (*c*) S. Ganss and B. Breit, *Angew. Chem., Int. Ed.*, 2016, **55**, 9738–9742; (*d*) P. Steib and B. Breit, *Angew. Chem., Int. Ed.*, 2018, **57**, 6572–6576; (*e*) C. Gagnon, É. Godin, C. Minozzi, J. Sosoe, C. Pochet and S. K. Collins, *Science*, 2020, **367**, 917–921.

11 For reviews on chiral *N*,*N*′-dioxides: (*a*) X. H. Liu, L. L. Lin and X. M. Feng, *Acc. Chem. Res.*, 2011, **44**, 574–587; (*b*) X. H. Liu, L. L. Lin and X. M. Feng, *Org. Chem. Front.*, 2014, **1**, 298–302; (*c*) X. H. Liu, H. F. Zheng, Y. Xia, L. L. Lin and X. M. Feng, *Acc. Chem. Res.*, 2017, **50**, 2621–2631; (*d*) X. H. Liu, S. X. Dong, L. L. Lin and X. M. Feng, *Chin. J. Chem.*, 2018, **36**, 791–797; (*e*) Z. Wang, X. H. Liu and X. M. Feng, *Aldrichimica Acta*, 2020, **53**, 3–10.

12 For selected reviews of *o*-QMs: (*a*) W.-J. Bai, J. G. David, Z.-G. Feng, M. G. Weaver, K.-L. Wu and T. R. R. Pettus, *Acc. Chem. Res.*, 2014, **47**, 3655–3664; (*b*) M. S. Singh, A. Nagaraju, N. Anand and S. Chowdhury, *RSC Adv.*, 2014, **4**, 55924–55959; (*c*) B. C. Yang and S. H. Gao, *Chem. Soc. Rev.*, 2018, **47**, 7926–7953.

13 For selected reviews of Friedel–Crafts alkylation of indoles: (*a*) M. Bandini, A. Melloni, S. Tommasi and A. Umani-Ronchi, *Synlett*, 2005, **8**, 1199–1222; (*b*) R. Dalpozzo, *Chem. Soc. Rev.*, 2015, **44**, 742–778; (*c*) I. P. Beletskaya and A. D. Averin, *Curr. Organocatal.*, 2016, **3**, 60–83; (*d*) J.-B. Chen and Y.-X. Jia, *Org. Biomol. Chem.*, 2017, **15**, 3550–3567.

14 For a selected review and book on medium-sized rings: (*a*) I. Shiina, *Chem. Rev.*, 2007, **107**, 239–273; (*b*) T. Janecki, in *Natural Lactones and Lactams: Synthesis, Occurrence and Biological Activity*, Wiley-VCH, Weinheim, 2013, pp. 193–227; for selected examples on medium-sized rings: (*c*) Z. J. Wu and J. Wang, *ACS Catal.*, 2017, **7**, 7647–7652; (*d*) Y. Wei, S. Liu, M.-M. Li, Y. Li, Y. Lan, L.-Q. Lu and W.-J. Xiao, *J. Am. Chem. Soc.*, 2019, **141**, 133–137.

15 For a selected review on the formation of macrocycles instead of medium rings, see: (*a*) J. S. Bradshaw, G. E. Maas, R. M. Izatt and J. J. Christensen, *Chem. Rev.*, 1979, **79**, 37–52, for selected examples of the formation of macrocycles instead of medium rings, see: (*b*) B. M. Trost and A. Quintard, *Angew. Chem., Int. Ed.*, 2012, **51**, 6704–6708; (*c*) A. W. H. Speed, T. J. Mann, R. V. O'Brien, R. R. Schrock and A. H. Hoveyda, *J. Am. Chem. Soc.*, 2014, **136**, 16136–16139; (*d*) Y. J. Zhou, P. Prediger, L. C. Dias, A. C. Murphy and P. F. Leadlay, *Angew. Chem., Int. Ed.*, 2015, **54**, 5232–5235; (*e*) W. Fu, L. H. Wang, Z. Yang, J.-S. Shen, F. Tang, J. Y. Zhang and X. L. Cui, *Chem. Commun.*, 2020, **56**, 960–963.

16 For selected reviews and examples of chiral discrimination: (*a*) X. X. Zhang, J. S. Bradshaw and R. M. Izatt, *Chem. Rev.*,

1997, **97**, 3313–3361; (*b*) L. Pu, *Chem. Rev.*, 2004, **104**, 1687–1716; (*c*) G. Uccello-Barretta, F. Balzano and P. Salvadori, *Curr. Pharm. Des.*, 2006, **12**, 4023–4045; (*d*) T. Ema, D. Tanida and T. Sakai, *J. Am. Chem. Soc.*, 2007, **129**, 10591–10596; (*e*) L.-L. Wang, Z. Chen, W.-E. Liu, H. Ke, S.-H. Wang and W. Jiang, *J. Am. Chem. Soc.*, 2017, **139**, 8436–8439; (*f*) H. X. Chai, Z. Chen, S.-H. Wang, M. Quan, L.-P. Yang, H. Ke and W. Jiang, *CCS Chem.*, 2020, **2**, 440–452.

17 For selected reviews: (*a*) R. P. Peng, Y. L. Xu and Q. Y. Cao, *Chin. Chem. Lett.*, 2018, **29**, 1465–1474; (*b*) Q. He, G. I. Vargas-Zúñiga, S. H. Kim, S. K. Kim and J. L. Sessler, *Chem. Rev.*, 2019, **119**, 9753–9835.

18 (*a*) CCDC 2016020 (**4aa**); ; (*b*) CCDC 2016694 (**3as**); ; (*c*) CCDC 2016695 (**4ab**) contains the ESI.†

19 J. R. Lakowicz, *Principles of Fluorescence Spectroscopy*, Kluwer Academic/Plenum, New York, 2nd edn, 1999.